International Journal of Science and Research (IJSR)
ISSN: 2319-7064
SJIF (2020): 7.803

Energy Consumption Optimization of Intelligent Reflecting Surface Assisted Mobile Edge Computing

Wenwu Xie[#1], Ruiren Xu[*2], Xin Peng[#3]

College of Information Science and Engineering, Hunan Institute of Science and Technology, Yue Yang, Hunan, China

[1]gavinxie [at]hnist.edu.cn
[2]xuruiren [at]foxmail.com
[3]Corresponding author Email: pengxin [at]hnist.edu.cn

This work was supported by the 135 Plan for Educational Science of Hunan Province under Grant XJK17BXX004

Abstract: ***For non-orthogonal multiple access (NOMA) assisted mobile edge computing (MEC) system, intelligent reflecting surface(IRS) is added to the system model, where power, phase shift and time allocation are jointly optimized to decrease the energy consumption of computational offloading. Closed-form expression of the optimal power and time allocation solution is obtained, and optimal phase shift is obtained. Then we can use it to determine whether orthogonal multiple access (OMA), pure NOMA or hybrid NOMA should be used conditions for MEC uninstallation. The simulation results show that the proposed optimization scheme can save the energy consumption of MEC offloading. Compared with the OMA effect, the performance is also improved.***

Keywords: non-orthogonal multiple access; intelligent reflecting surface; mobile edge computing

1. Introduction

With the advent of the Internet of Everything era, the explosive growth of the number of mobile users and devices will lead to a sharp increase in data to be processed. However, because of devices' limited computing power, they cannot well support resource-intensive applications. To solve this problem, powerful computing nodes are arranged at the network edge, and big data generation and storage are migrated to the network edge nodes. Encouraged by these trends, many studies have proposed combining NOMA and MEC to improve the performance of MEC systems. To guarantee outstanding network operation, MEC is standardized by the European Telecommunications Standards Institute (ETSI) industry specification group. Compared with traditional cloud computing, MEC pushes cloud computing functions from the core network to edge nodes in the wireless access network to reduce propagation delay. In addition, the typical MEC is to computing triage from the user's point of view. Mobile user equipment benefits from the powerful computing capabilities of the MEC server, which can expedite task calculations and optimize energy consumption. As an important technology for architecture optimization, MEC can also be regarded as a key research direction for the development of 5G networks and the Internet of Things. Because the MEC calculation of the offloading link is far from perfect, its potential has not yet been fully utilized. For example, devices located at the edge of a cell usually have a low offload success rate. At this time, compared with local computing, their computing offloading may require more waiting time and energy. Therefore, the compulsory maintenance of these devices depends on their own computing resources, but this often fails to support resource-intensive applications. From the communications point of view, it must be improved to offload performance of the MEC system.

Power domain NOMA is a common solution today. In this solution, continuous interference (SIC) technology is applied to the receiver, and users with large channel gains can use it to eliminate interference from users with small channel gains. Compared with OMA, multiple users can transmit signals at the same time with lower interference. Because of the high spectrum efficiency, compared OMA, NOMA's resource optimization can obtain better performance in the case of overall system rate and energy efficiency. Because the performance of NOMA is better than that of OMA, in order to transmit signals with lower interference, NOMA uplink and downlink can be used in MEC network to bear more users. Although NOMA-MEC has many advantages, there are still some challenges consisting of resource allocation, reliability, security and privacy.

MEC with NOMA in [1, 2] has been considered as significant technologies in wireless networks. The complex optimization framework in [3, 4] shows that not only can applying NOMA to MEC avoid serious delays, but also reduce consumption of energy. The analysis consequent in [5] was confirmed that there are some advantages of NOMA-MEC offloading by using fixed bandwidth allocation. In the latest work [6, 7], the application of IRS on the MEC system is deemed as one of the feasible solutions that can make MEC in the offloading phase beneficial. The calculation delay and energy consumption are regarded as the performance indicators for evaluating the IRS-assisted MEC system in [6, 7]. These methods only use the advantages of IRS to reduce the calculation delay of the MEC system and improve energy efficiency. In literature [8], in order to optimize the system energy consumption in NOMA-MEC, the offloading task and offloading success rate level of each user and the SIC decoding sequence are optimized. In addition, in literature [9], we maximize energy consumption by optimizing the transmission power. In order to explore the advantages of IRS in wireless communication, people have done a lot of research on its ergodic capacity analysis [10], channel estimation [11], actual reflection phase shift modeling [12], and phase shift design. On the premise of maintaining the target received signal-to-noise ratio [13], a joint design scheme based on IRS phase shift and AP precoding is proposed to minimize the transmission power based on the complex technology of semi-definite relaxation and alternate optimization. These studies were subsequently extended to discrete phase shift settings [14]. These impressive studies have inspired the discovery of the role of IRS in the MEC system.

In addition, the total computational data is considered as an important performance indicator for assessing the overall calculating power of the MEC system. Although the existing MEC system in [8, 9] utilizes the total number of calculations or maximizes the computational efficiency, these works have not yet studied the performance of IRS to the MEC system. Therefore, there are not many research in the application of IRS in improving computational shunting. Few documents have considered the energy consumption optimization problem in the IRS-assisted NOMA-MEC system, which encouraged motivated the work of this paper.

In order to gain a deep understanding of NOMA-MEC, this article focuses on two basic planned user cases to research the effect of IRS aided NOMA-MEC offloading. The actual studies in [3-5] only considered two mobile offloading tractrices, namely pure NOMA OMA and OMA (i.e., providing services for users at the same time without giving users extra time). This paper proposes another scheme called hybrid NOMA, where a user first transfers part of the task by using a time slot distributed to other user, then transfers the remaining tasks in its own exclusive time slot. This paper studies the performance of these three strategies, and obtains a closed-form expression of the phase shift optimization scheme, the optimal time and power allocation solution through the application of geometric programming (GP). Not only can these closed-form solutions show significant features of NOMA-MEC offloading promote low-complexity resource allocation, but also reduce complexity resource allocation. For example, when the user has a high demand for task offloading delay, hybrid NOMA-MEC is certified to be better than OMA-MEC by using the obtained closed-form solution. However, if the user's task has a delay tolerance, OMA-MEC is preferred. It is worth noting that in both cases, the pure NOMA schedule is not the first choice.

2. System Model

This article considers the IRS-assisted MEC system shown in Figure 1. The model consists of k users $(1,\ldots,K)$, an IRS and a base station equipped with an MEC server. The IRS is deployed to assist in the deployment of computing tasks from K users to MEC base stations. The IRS has R reflective sub-surfaces, and each sub-surface contains M elements. $\mathbf{\Theta} \triangleq diag\left(e^{j\omega_1},\ldots,e^{j\omega_R}\right) \in \mathbb{C}^{R\times R}$ represents the IRS diagonal reflection matrix, where, for simplicity, the reflection amplitude of each sub-surface is set to 1, and, ω_r , $r \in \{1,\ldots,R\}$ represents the phase shift of the sub-surface R.

The article considers an IRS-MEC offloading scheme, where K users those have different quality of service requirements need to communicate with an access point equipped with a MEC server through a direct link and an IRS reflection link. Due to its limited computing power, it is assumed that the user chooses to offload its computationally intensive, delay-critical, indivisible tasks to the server.

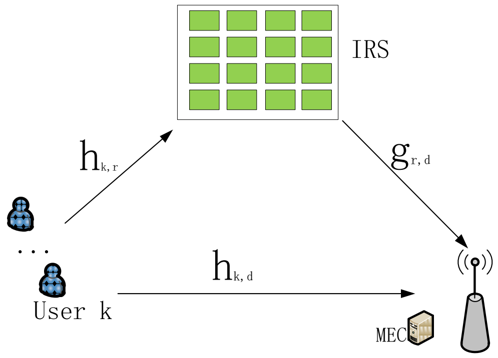

Figure 1: System Model

The task data transmitted by each user is denoted as N_k , and the calculation delay of the transmission task is denoted as $D_k,(k=1,...,K)$ .Because of generality, we suppose that $N_k = N,(k=1,...,K)$, and sort users according to their calculation delay (i.e. $D_1 \le \ldots \le D_K$). It is supposed that only two users the are managed by MEC server, namely user a and user b, $a \le b$, to perform services on the same resource block in order to low system complexity. It is worth noting that which manages two users to perform NOMA is consistent with implementing NOMA in LTE-A. OMA-MEC is also first explained to better explain the benefits of NOMA. When the user uninstalls, the signal received by MEC is expressed as

$$y = \left(h_a + \mathbf{g}_{r,d}^T \mathbf{\Theta} \mathbf{h}_{a,r}\right)\sqrt{P}x_a + \left(h_b + \mathbf{g}_{r,d}^T \mathbf{\Theta} \mathbf{h}_{b,r}\right)\sqrt{P}x_b + n \quad (1)$$

Paper ID: SR211214135044 DOI: 10.21275/SR211214135044

where $\boldsymbol{\Theta} \triangleq diag\left(e^{j\omega_1}, \ldots, e^{j\omega_R}\right) \in \mathbb{C}^{R\times R}$ representsthe reflection-coefficient matrix of the IRS, then $\mathbf{g}_{r,d} = \left[\mathbf{g}_{1,d}\ \mathbf{g}_{2,d}\ \ldots\ \mathbf{g}_{R,d}\right]^T$, $i \in \{a,b\}$ represents the single-antenna fading channel between the rth reflective surface of the IRS and the MEC. $\mathbf{h}_{i,r} = \left[\mathbf{h}_{i,1}\ \mathbf{h}_{i,2}\ \ldots\ \mathbf{h}_{i,R}\right]^T$, $i \in \{a,b\}$ represents the fading channel between the rth reflective surface of the IRS and the single-antenna user, $h_i, i \in \{a,b\}$ represents the direct link from user i to the MEC.

Then h_i, $\mathbf{h}_{i,r}$ and $\mathbf{g}_{r,d}$ are Rayleigh distributed random variables and are independent of each other.

If OMA is used, each user will be distributed a dedicated time slot for offloading. Because the delay of user a is shorter than the delay required by user b, user a is provided services first. Therefore, when the noise is 1, the user transmits power denoted by P_a^{OMA} and P_b^{OMA} needs to meet

$$D_a \ln\left(1 + P_a^{OMA} \left|\mathbf{H}_a\right|^2\right) = N \tag{2}$$

$$\left(D_b - D_a\right)\ln\left(1 + P_b^{OMA} \left|\mathbf{H}_b\right|^2\right) = N \tag{3}$$

where $\mathbf{H}_i = h_i + \mathbf{g}_{r,d}^T \boldsymbol{\Theta} \mathbf{h}_{i,rb}$ represents the channel gain of user i, $i \in \{a,b\}$.

Two users can offload their tasks to the server at the same time D_a by using the principle of NOMA. It is important to note that if user a is decoded in the second phase of SIC and the data rate constraint of use bis

$$R_b \le \ln\left(1 + \frac{P_{b,1}\left|\mathbf{H}_b\right|^2}{\left|\mathbf{H}_a\right|^2 + 1}\right) \tag{4}$$

where $P_{b,1}$ represents the power which is used by user b during D_a .When decoding is performed in the next step, its performance is the same as that of OMA.

It was pointed out in [5] that if the user completely depends on D_a, compared in OMA, then user b was required to deplete more energy in NOMA. Therefore, we study hybrid NOMA, i.e., user b and user a share D_a, and then after D_a, continuously send another time interval represented by T_b. $P_{b,2}$ represents the power used by user b during T_b. The experience of user a is the same as that of OMA, so this article only focuses on the performance of the user b.

3. IRS-assisted MEC offloading

The IRS-MEC offloading energy consumption minimization problem can be expressed as:

$$\min_{\Theta, T_b, P_{b,1}, P_{b,2}} D_a P_{b,1} + T_b P_{b,2} \tag{5a}$$

$$\begin{aligned} s.t.\ & D_a \ln\left(1 + \frac{P_{b,1}\left|\mathbf{H}_b\right|^2}{P_a^{OMA}\left|\mathbf{H}_a\right|^2 + 1}\right) \\ & + T_b \ln\left(1 + P_{b,2}\left|\mathbf{H}_b\right|^2\right) \ge N \end{aligned} \tag{5b}$$

$$0 \le T_b \le D_b - D_a \tag{5c}$$

$$P_{b,i} \ge 0, \forall i \in \{1,2\} \tag{5d}$$

(5a) represents the user b's MEC offloading energy consumption, (5b) represents the rate constraint to ensure that the data N of user b is offloaded within $D_a + T_b$, and (5c) represents the delay constraint, namely $D_a + T_b \le D_b$. It is worth noticing that for the case $D_a = D_b$, the benefits of using NOMA are evident, in which the power in NOMA is limited, while the power needed for the OMA case becomes unlimited.

Firstly, in order to avoid trivial situations with OMA solutions, this article will focus on the scenarios ($D_b < 2D_a$).Specially, by applying geometric programming, we first acquire the optimal solution of $P_{b,1}$ and $P_{b,2}$ as a function of T_b, and then see the optimal solution of T_b. The scene $D_b \ge 2D_a$ will also be studied at the end of this essay.

A. Power optimization program

The fixed phase shift is a constant $\left|\mathbf{H}_b\right|$. Next, in order to make the geometric planning applicable, the objective function and constraints need to be converted as follows. By using $D_a \ln\left(1 + P_a^{OMA}\left|\mathbf{H}_b\right|^2\right) = N$, the constraint (5b) can be written as follows:

$$\ln\left(1+e^{-\frac{N}{D_b}}P_{b,1}\left|\mathbf{H}_b\right|^2\right)^{D_a} \times\left(1+P_{b,2}\left|\mathbf{H}_b\right|^2\right)^{T_b} \geq N \quad (6)$$

Define $x_1 = 1+e^{-N/D_a}P_{b,1}\left|\mathbf{H}_b\right|^2$, $x_2 = 1+P_{b,2}\left|\mathbf{H}_b\right|^2$, the question (1) became the following equivalent form:

$$\min_{T_b,P_{b,1},P_{b,2}} D_a e^{\frac{N}{D_a}}\left(x_1-1\right)\left|\mathbf{H}_b\right|^{-2}+T_b\left(x_2-1\right)\left|\mathbf{H}_b\right|^{-2} \quad (7a)$$

$$s.t.\ e^N x_1^{-D_a} x_2^{-T_b} \leq 1 \quad (7b)$$

$$0 \leq T_b \leq D_b - D_a \quad (7c)$$

$$x_i \geq 1, \forall i \in \{1,2\} \quad (7d)$$

Because $\left|\mathbf{H}_b\right|$, D_a, Nare all constants, the above problem(7a) can be abbreviated as

$$\min_{T_b,P_{a,1},P_{b,2}} D_a e^{\frac{N}{D_a}} x_1\left|\mathbf{H}_b\right|^{-2}+T_b\left(x_2-1\right)\left|\mathbf{H}_b\right|^{-2} \quad (8)$$

Define $y_i = \ln x_i, i=1,2$. The problem can be converted to the following form by using fixed T_b

$$\min_{y_1,y_2} D_a e^{\frac{N}{D_a}+y_1}\left|\mathbf{H}_b\right|^{-2}+T_b\left(e^{y_2}-1\right)\left|\mathbf{H}_b\right|^{-2} \quad (9a)$$

$$s.t.\ e^{N-y_1D_a-y_2T_b} \leq 1 \quad (9b)$$

$$y_i \geq 0, \forall i \in \{1,2\} \quad (9c)$$

The function of the above problem is

$$\begin{aligned} &L\left(y_1,y_2,\lambda_1,\lambda_2,\lambda_3\right) \\ &= D_a e^{\frac{N}{D_a}+y_1}\left|\mathbf{H}_b\right|^{-2}+T_b\left(e^{y_2}-1\right)\left|\mathbf{H}_b\right|^{-2} \\ &-\lambda_1 y_1-\lambda_2 y_2+\lambda_3\left(N-y_1D_a-y_2T_b\right) \end{aligned} \quad (10)$$

So, the KKT condition at this time is

$$\begin{cases} D_a e^{\frac{N}{D_a}+y_1}\left|\mathbf{H}_b\right|^{-2}-\lambda_1-\lambda_3 D_a = 0 \\ T_b e^{y_2}\left|\mathbf{H}_b\right|^{-2}-\lambda_2-\lambda_3 T_b = 0 \\ N-y_1D_a-y_2T_b \leq 0 \\ \lambda_3\left(N-y_1D_a-y_2T_b\right)=0 \\ y_i \geq 0, \forall i \in \{1,2\} \\ \lambda_i y_i = 0, \forall i \in \{1,2\} \\ \lambda_i \geq 0, \forall i \in \{1,2,3\} \end{cases} \quad (11)$$

And because $D_b < 2D_a, T_b \leq D_b - D_a < D_a$, y_i^* satisfies $y_i > 0$, this means that the solution in (14) is viable. By using the power allocation solution in (10), the optimal solution of $P_{b,1}$ and $P_{b,2}$ in the problem (1) can be denoted as the closed-form functions

$$P_{b,1}^* = \left|\mathbf{H}_b\right|^{-2} e^{\frac{N}{D_a}}\left(e^{\frac{N(D_a-T_b)}{D_a(D_a+T_b)}}-1\right) \quad (12)$$

$$P_{b,2}^* = \left|\mathbf{H}_b\right|^{-2}\left(e^{\frac{N(D_a-T_b)}{D_a(D_a+T_b)}+\frac{N}{D_a}}-1\right) \quad (13)$$

$\left|\mathbf{H}_b\right|$ is the larger, the smaller the allocated power, the energy consumption will also be reduced.

Proof: Appendix A.

B. Phase shift optimization

First, optimize the IRS phase shift for different unloading periods. In order to ensure the throughput and fairness of the entire system, in the NOMA system, users with good channel conditions have less power allocation at the transmitting end than users with poor channel conditions. For the process of offloading tasks for different users, the better the channel conditions, the lower the energy consumption, so the problem (5) can be solved by solving the following problems:

$$\begin{aligned} &\max_{\Theta} \left|h_b+\mathbf{g}_{r,d}^T\mathbf{\Theta}\mathbf{h}_{b,r}\right|^2 \\ &s.t.\ \left|\exp\left(j\alpha_{k,b}\right)\right|=1 \\ &\alpha_{k,b} \in [0,2\pi], \forall k \in [1,N] \end{aligned} \quad (14)$$

We can modify the objective function of the above formula to get

$$\left|h_b+\mathbf{g}_{r,d}^T\mathbf{\Theta}\mathbf{h}_{b,r}\right| = \left|h_b+\mathbf{\theta}_b\mathbf{b}_b\right| \quad (15)$$

where $\mathbf{b}_b = diag\left(\mathbf{g}_b\right)h_{br}$, $\theta_k = \left[\theta_{k,1},\ldots,\theta_{k,N}\right] = \left[\exp\left(j\alpha_{k,1}\right),\ldots,\exp\left(j\alpha_{k,N}\right)\right]$, $\left|\mathbf{\theta}_{k,b}\right|=1$.Next, the upper limit of the above formula can be derived as $\left|h_b+\mathbf{\theta}_b\mathbf{b}_b\right| \leq \left|h_b\right|+\sum_{n=1}^N\left|\mathbf{\theta}_{k,n}\mathbf{b}_k[n]\right| = \left|h_b\right|+\sum_{n=1}^N\left|\mathbf{b}_k[n]\right|$ by using the triangle inequality, where $\mathbf{b}_k[n]$ is the nth element of $\mathbf{b}_k$, for $n \in [1,N], \left|\theta_{k,n}\right|=1$. We can get the upper limit through

$$a_{k,n} = \arg\left(h_b\right)-\arg\left(\mathbf{b}_k[n]\right) \quad (16)$$

where $\arg(*)$ represents the phase operator. Therefore, the best phase shift vector θ_k^* can be achieved from equation (19), and then the best phase shift matrix Θ_k^* can be achieved.

Through some mathematical operations, $\left|h_b + \mathbf{g}_{r,d}^T \boldsymbol{\Theta} \mathbf{h}_{b,r}\right|^2$ can be written as

$$\begin{aligned}&\left|h_b + \mathbf{g}_{r,d}^T \boldsymbol{\Theta} \mathbf{h}_{b,r}\right|^2 = \left|h_b\right|^2 + \left|\mathbf{g}_{r,d}^T \boldsymbol{\Theta} \mathbf{h}_{b,r}\right|^2 \\ &+2\left|\mathbf{g}_{r,d}^T \boldsymbol{\Theta} \mathbf{h}_{b,r}\right|\left|h_b\right|\cos\left[\arg\left(h_b\right) - \arg\left(\mathbf{g}_{r,d}^T \boldsymbol{\Theta} \mathbf{h}_{b,r}\right)\right]\end{aligned} \quad (17)$$

By formula (20), if $\left|h_b + \mathbf{g}_{r,d}^T \boldsymbol{\Theta} \mathbf{h}_{b,r}\right|^2$ get the maximum value, $\cos\left[\arg\left(h_b\right) - \arg\left(\mathbf{g}_{r,d}^T \boldsymbol{\Theta} \mathbf{h}_{b,r}\right)\right] = 1$. This shows that the phases of the direct link and the cascaded link between the nth device and the AP are the same, i.e., $\arg\left(h_b\right) = \arg\left(\mathbf{g}_{r,d}^T \boldsymbol{\Theta} \mathbf{h}_{b,r}\right)$. Therefore, the optimal phase shift matrix aligns the cascade link between the K devices and the AP with the direct link through the IRS. It can be expressed as, $\mathbf{g}_{r,d}^T \boldsymbol{\Theta} \mathbf{h}_{b,r} = \xi_b h_b, \forall k \in [1, K]$, where ξ_b is a positive scalar coefficient.

By using the above, the following description is needed to quantify the signal intensity of the information reflection during the unloading phase.

Compared with devices without IRS, deploying IRS can increase the received signal power of the nth device at most $(1+\xi_b)^2$ during the offloading phase of the nth device. Besides, the signal strength ξ_n of the nth device is proportional to the quantities of reflective elements of the IRS. Therefore, significant improvements can be made in the offloading stage by increasing the number of reflective elements. So, we can get

$$\left|h_b + \mathbf{g}_{r,d}^T \boldsymbol{\Theta} \mathbf{h}_{b,r}\right|^2 \le (1+\xi_b)^2 \left|h_b\right|^2 \quad (18)$$

C. Time delay optimization scheme

By replacing the optimal solution obtained in the above formula with (5), the original problem can be shown in an equivalent form as below:

$$\min_{T_b} g_{T_b} = D_a e^{\frac{N}{D_a}} \left(e^{y_1^*} - 1\right) + T_b \left(e^{y_2^*} - 1\right) \quad (19a)$$

$$s.t. \quad T_b \le D_b - D_a \quad (19b)$$

whereby g_{T_b} omitting the constant $\left|h_b\right|^{-2}$ in the initial objective function, the energy consumption is standardized. y_1^* and y_2^* are both functions of T_b.

The derivative with g_{T_b} respect to T_b can be written as:

$$\begin{aligned}\frac{dg_{T_b}}{dT_b} &= D_a e^{\frac{N}{D_a}} e^{y_1^*} \frac{(-2N)}{(D_a + T_b)^2} \\ &+ \left(e^{y_2^*} - 1\right) + T_b e^{y_2^*} \frac{(-2N)}{(D_a + T_b)^2}\end{aligned} \quad (20)$$

And $y_2^* = y_1^* + N/D_a$. Therefore, the derivative of g_{T_b} can be expressed as:

$$\begin{aligned}\frac{dg_{T_b}}{dT_b} &= D_a e^{y_2^*} \frac{(-2N)}{(D_a + T_b)^2} \\ &+ \left(e^{y_2^*} - 1\right) + T_b e^{y_2^*} \frac{(-2N)}{(D_a + T_b)^2} \\ &= e^{y_2^*}\left(1 - \frac{2N}{D_a + T_b}\right) - 1\end{aligned} \quad (21)$$

In addition, $y_2^* = N\left(D_a - T_b\right)/D_a\left(D_a + T_b\right) + N/D_a = 2N/D_a + T_b$. Therefore, the derivative of g_{T_b} can be written as:

$$\frac{dg_{T_b}}{dT_b} = g_x\left(\frac{2N}{D_a + T_b}\right) \quad (22)$$

where $g_x @ e^x (1-x) - 1$. For some reason that for $x \ge 0, dg_x(x)/dx = -xe^x \le 0$, $g_x(x)$ is a monotonic non-increasing function. And because $dg_{T_b}/dT_b \le g_x(0) = 0$, $dg_{T_b}/dT_b \le 0$. This means g_{T_b} monotonically non-increasing. Therefore, the optimal solution of T_b for problem (5) is written as following equation;

$$T_b^* = D_b - D_a \quad (23)$$

It is worth noting that because of consideration in this part $D_b < 2D_a$, $T_b^* < D_a$.

On NOMA's performance over OMA: It can be proved that as shown below, OMA cannot be better than NOMA. The energy consumption difference between NOMA-MEC and

OMA-MEC

$$\Delta_1 @ D_a e^{\frac{N}{D_a}}\left(e^{y_1^*}-1\right)\left|\mathbf{H}_b\right|^{-2} + T_b\left(e^{y_2^*}-1\right)\left|\mathbf{H}_b\right|^{-2} - T_b\left(e^{\frac{N}{T_b}}-1\right)\left|\mathbf{H}_b\right|^{-2} \quad (24)$$

The difference can also be written as:

$$\begin{aligned}\left|\mathbf{H}_b\right|^2 \Delta_1 @ D_a e^{y_2^*}\left(D_a+T_b\right) - D_a e^{\frac{N}{D_a}} - T_b e^{\frac{N}{T_b}} \\ = e^{\frac{2N}{D_a+T_b}}\left(D_a+T_b\right) - D_a e^{\frac{N}{D_a}} - T_b e^{\frac{N}{T_b}} \quad (25) \\ = f_{T_b}\left(T_b\right)\end{aligned}$$

Note that for $x < D_a$, $f_{T_b}\left(T_b\right)$ isa monotonic non-decreasing function. The derivative of $f_{T_b}\left(T_b\right)$ is written as:

$$\frac{df_{T_b}(x)}{dx} = e^{\frac{2N}{D_a+x}}\left(1-\frac{2N}{D_a+x}\right) - e^{\frac{N}{x}}\left(1-e^{\frac{N}{x}}\right) \quad (26)$$

Define $f_y(y) = e^{N/y}(1-N/y)$, the derivative of $f_{T_b}(x)$ can be written as:

$$\frac{df_{T_b}(x)}{dx} = f_y\left(\frac{D_a+x}{2}\right) - f_y(x) \quad (27)$$

Because $df_y(y)/dy = N^2 e^{N/y}/y^3 > 0$, $f_y(y)$ is a monotonically increasing function. $(D_a+x)/2 > x$ since $x < D_a$ .Hence, the derivative $f_{T_b}(x)$ is a non-negative number as follows:

$$\frac{df_{T_b}(x)}{dx} = f_y\left(\frac{D_a+x}{2}\right) - f_y(x) \ge 0 \quad (28)$$

This means that $f_{T_b}(x)$ is a monotonic non-decreasing function. Because $T_b < D_a$, we can get

$$f_{T_b}\left(T_b\right) \le f_{T_b}\left(D_a\right) = 0 \quad (29)$$

In combination with the above, hybrid NOMA, obtained solution with $\lambda_i = 0, \forall i \in \{1,2\}$ generates the least energy. By using (32), the required power during D_a and T_b can be obtained and proved to be complete.

Moreover, $f_{T_b}\left(T_b\right) \le 0$ this means that under the conditions of $D_b < 2D_a$, the performance of using NOMA is better than or at least the same as OMA. In comparison, the situation $D_b \ge 2D_a$: this situation corresponds to a scenario where the user b has less delay requirements. For the case $D_b \ge 2D_a$, because $T_b = D_b - D_a$, T_b can be greater than D_a. The OMA produces the optimal property in this case, as shown below. Since only when $T_b < D_a$ and hybrid NOMA energy consumption, i.e., g_{T_b} is a monotonic non-increasing function of T_b, the optimal solution of power is feasible. So g_{T_b} always strictly restricted by the lower bound

$$D_a\left(e^{\frac{N}{D_a}}-1\right)\left|\mathbf{H}_b\right|^{-2} \quad (30)$$

On the other hand, when $D_b \ge 2D_a$, as shown in (23), $\lambda_1 \ne 0, \lambda_2 = 0$, the lower limit of equation (33) can be realized through OMA. In other words, at that time $D_b \ge 2D_a$, the energy consumption of OMA was less than that of hybrid NOMA. In addition, OMA can be superior to pure NOMA because

$$\begin{aligned}&\frac{E_{OMA}-E_{NOMA}}{\left|\mathbf{H}_b\right|^{-2}} \\ &\underset{a}{\le} D_a\left(e^{\frac{N}{D_a}}-1\right) - D_a e^{\frac{N}{D_a}}\left(e^{\frac{N}{D_a}}-1\right) \quad (31) \\ &= -D_a\left(e^{\frac{N}{D_a}}-1\right)^2 \le 0\end{aligned}$$

where because the minimum energy demanded by OMA is more than the lower limit, step (a) can be run. Therefore, it can be noted that OMA performance is better than hybrid NOMA and pure NOMA at that time $D_b \ge 2D_a$. Because more relaxed relays make using only interference-free time slots ($D_b - D_a$) for offloading to be probable, this completion is reasonable.

4. Result Analysis

In this section, the performance raised IRS-assisted MEC scheme will be assessed through simulation results, in which normalized energy consumption is used. This paper considers describing network connections in two dimensions. The network model consists of two users, an IRS and a base station equipped with a MEC server. The channel model between user and IRS, IRS and base station, and user and base station are all Rayleigh channels. In addition, the reflections element of IRS is 50, the system bandwidth is 1, the noise power is set to 1, and the reflection amplitude of IRS sub-surface is set to 1. The following sections detail the simulation results of this paper, including the performance of the proposed optimization and multi-device scenarios in various transport modes. Under the same configuration, the proposed scheme is compared with the existing benchmark scheme: NOMA/OMA transport scheme; Transmission power of different users under NOMA.

First, this paper evaluates and compares the performance of the device during uninstallation between NOMA-MEC and OMA-MEC at Da=20, as shown in Fig2. Because OMA-MEC uses a short cycle ($D_b - D_a$) for offloading. As can be seen from Fig.2, the use of IRS-assisted NOMA-MEC could significantly improve performance than IRS-assisted OMA-MEC, especially when D_b is smaller. For example, $D_b \to D_a$, ($D_b - D_a$) nears zero. Therefore, as shown in the fig2, the energy consumption in IRS-assisted OMA-MEC becomes too large. On the other hand, not only do IRS-assisted NOMA-MEC use ($D_b - D_a$) for offloading but during D_a, which makes the energy consumption in IRS-assisted NOMA-MEC more stable.

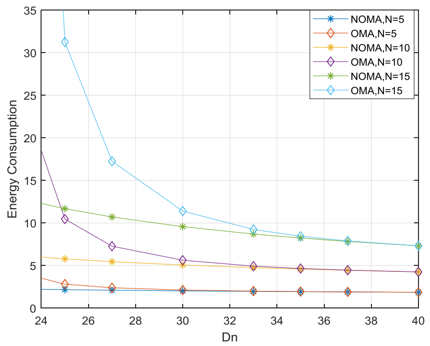

Figure 2: Performance comparison between IRS-assisted NOMA-MEC and IRS-assisted OMA-MEC when Da=20

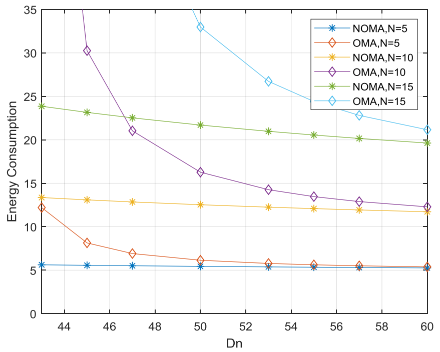

Figure 3: Performance comparison between IRS-assisted NOMA-MEC and IRS-assisted OMA-MEC when Da=40

In addition, the comparison between Fig2 and Fig3 shows D_a the impact on energy consumption when D_a set to 20 and 40 respectively. On the other hand, in a fixed situation $D_b - D_a$, by increasing D_a, NOMA-MEC has more time to offload data by increasing D_a, which helps to reduce energy consumption, as shown in Fig2 and Fig3. When D_a increases, the energy consumption of NOMA-MEC is getting closer and closer to the energy consumption of OMA-MEC. This is because with D_b increasing, user b will have more time delay to transmit tasks, so that it can transmit in time $D_b - D_a$ .Fig4 provides more detailed information on the different $P_{b,1}$ and $P_{b,2}$ aspects. At this time, this article sets $D_a = 20$, N=5, 10, 15. It can be seen from the fig3 that when D_b increases, the power distributed to D_a is close to zero, which means that performance of hybrid NOMA is getting closer and closer to OMA.

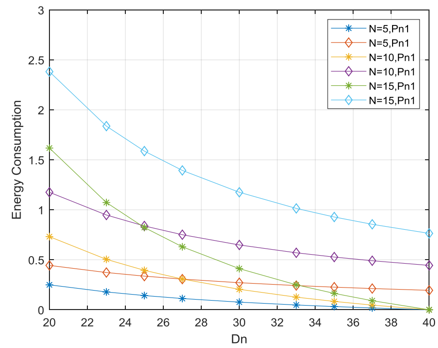

Figure 4: The performance of IRS-assisted NOMA-MEC when Da=20

5. Summarize

In this paper, the principle of NOMA is used for IRS-assisted MEC, and the optimal solution of power and time allocation is obtained through GP, and the optimal phase shift scheme is obtained at the same time. We also obtain analysis and simulation results, which proves that in IRS-assisted MEC, compared with traditional OMA and pure NOMA, the MEC offloading performance of hybrid NOMA is superior. In this article, it is assumed that considering the use of multiple access points as MEC cloud is an important topic for future research [7], a single access point serves as the MEC server. As more access points serve many users, the complexity of implementing NOMA and MEC combinations may become too high, which will stimulate the use of advanced method such as machine learning and game theory in [8, 9]. In addition, this article assumes ideal channel state information (CSI) and studying the influence of imperfect CSI for the raised algorithm is an important topic of research.

Appendix A

The first is for hybrid NOMA, because $\lambda_i = 0, \forall i \in \{1,2\}, y_i > 0$, therefore, $P_{b,1}$ and $P_{b,2}$ are not zero, which is why this situation is called hybrid NOMA. On this situation, we could certify $\lambda_3 \le 0$ as follows. If $\lambda_3 = 0$, then the KKT condition leads to the following two equations:

$$\begin{cases} D_a e^{\frac{N}{D_a}+y_1} \left|\mathbf{H}_b\right|^{-2} = 0 \\ T_b e^{y_2} \left|\mathbf{H}_b\right|^{-2} = 0 \end{cases} \quad \text{(a)}$$

This cannot be true. Therefore, $\lambda_3 \neq 0$, this can rewrite the KKT condition as

$$\begin{cases} D_a e^{\frac{N}{D_a}+y_1} \left|\mathbf{H}_b\right|^{-2} - \lambda_3 D_a = 0 \\ T_b e^{y_2} \left|\mathbf{H}_b\right|^{-2} - \lambda_3 T_b = 0 \\ N - y_1 D_a - y_2 T_b = 0 \\ y_i > 0, \forall i \in \{1,2\} \end{cases} \quad \text{(b)}$$

Through some algebraic operations, the best solution of y_1 and y_2 can be obtained as shown below:

$$\begin{cases} y_1^* = \dfrac{N\left(D_a - T_b\right)}{D_a\left(D_a + T_b\right)} \\ y_2^* = \dfrac{N\left(D_a - T_b\right)}{D_a\left(D_a + T_b\right)} + \dfrac{N}{D_a} \end{cases} \quad \text{(c)}$$

Then substituting it into the relational expression of x, the optimal solution of $P_{b,1}$ and $P_{b,2}$ can be obtained.

References

[1] Ding Z, Lei X, Karagiannidis G K, et al. A Survey on Non-Orthogonal Multiple Access for 5G Networks: Research Challenges and Future Trends [J]. IEEE Journal on Selected Areas in Communications, 2017, PP (99):1-1.
[2] Khan A R, Othman M, Madani S A, et al. A Survey of Mobile Cloud Computing Application Models [J]. Communications Surveys & Tutorials, IEEE, 2014, 16(1):393-413.
[3] Wang F, Xu J, Ding Z. Multi-Antenna NOMA for Computation Offloading in Multiuser Mobile Edge Computing Systems [J]. IEEE Transactions on Communications, 2019, 67(3):2450-2463.
[4] Kiani A, Ansari N. Edge Computing Aware NOMA for 5G Networks [J]. IEEE Internet of Things Journal, 2017, PP (99):1-1.
[5] Ding Z, Fan P, Poor H V. Impact of Non-orthogonal Multiple Access on the Offloading of Mobile Edge Computing [J]. IEEE Transactions on Communications, 2018:1-1.
[6] T. Bai, C. Pan, Y. Deng, M. Lakshman, A. Mullainathan and L. Hanzo, "Latency Minimization for Intelligent Reflecting Surface Aided Mobile Edge Computing, " in IEEE Journal on Selected Areas in Communications, vol. 38, no. 11, pp. 2666-2682, Nov. 2020.
[7] T. Bai, C. Pan, H. Ren, Y. Deng, M. Lakshman and A. Mullainathan, "Resource Allocation for Intelligent Reflecting Surface Aided Wireless Powered Mobile Edge Computing in OFDM Systems, " in IEEE Transactions on Wireless Communications, vol. 20, no. 8, pp.5389-5407, Aug.2021.
[8] Zhou F, Wu Y, Hu R Q, et al. Computation Rate Maximization in UAV-Enabled Wireless Powered Mobile-Edge Computing Systems [J]. IEEE Journal on Selected Areas in Communications, 2018, 36(9):1927-1941.
[9] F. Zhou and R. Q. Hu, "Computation Efficiency Maximization in Wireless-Powered Mobile Edge Computing Networks, " in IEEE Transactions on Wireless Communications, vol. 19, no. 5, pp. 3170-3184, May 2020.
[10] Han Y, Tang W, Jinn S, et al. Large Intelligent Surface-Assisted Wireless Communication Exploiting Statistical CSI [J]. IEEE Transactions on Vehicular Technology, 2019, PP (99):1-1.
[11] Zheng B, Zhang R. Intelligent Reflecting Surface-Enhanced OFDM: Channel Estimation and Reflection Optimization [J]. IEEE Wireless Communication Letters, 2019, PP (99):1-1.
[12] S. Abeywickrama, R. Zhang, Q. Wu and C. Yuen, "Intelligent Reflecting Surface: Practical Phase Shift Model and Beamforming Optimization, " in IEEE Transactions on Communications, vol. 68, no. 9, pp. 5849-5863, Sept. 2020.
[13] Wu Q, ZhangR. Intelligent Reflecting Surface Enhanced Wireless Network via Joint Active and Passive Beamforming [J]. IEEE Transactions on Wireless Communications, 2019, PP (99):1-1.
[14] Wu Q, ZhangR. Beamforming Optimization for Wireless Network Aided by Intelligent Reflecting Surface with Discrete Phase Shifts [J]. IEEE Transactions on Communications, 2020, 68(3):1838-1851.
[15] Z. Ding, J. Xu, O. A. Dobre and H. V. Poor, "Joint Power and Time Allocation for NOMA–MEC Offloading, " in IEEE Transactions on Vehicular Technology, vol. 68, no. 6, pp. 6207-6211, June 2019.

Author Profile

Wenwuxie (1979-), Male, Associate Professor, Ph.D., the main research direction is non-orthogonal multiple access technology, intelligent reflector technology. Email: gavinxie@hnist.edu.cn

Ruiren Xu (1996-), Male, Graduate Student, main research direction is intelligent reflective surface, mobile edge computing. Email: xuruiren@foxmail.com

Xin Peng (1981-), Male, Professor, Ph.D., the main research direction is car networking, edge computing. Email: pengxin@hnist.edu.cn